April 2011

The Photophysical Properties of a Symmetrically Substituted 2,5 ¨C Diarylidene Cyclopentanone Dye: (2E,5E)©2,5©

Katarina Lynn Lopez
Worcester Polytechnic Institute

The Photophysical Properties of a Symmetrically Substituted 2,5 – Diarylidene Cyclopentanone Dye: (2E,5E)-2,5-bis(4-methoxycinnamylidene)-cyclopentanone

A Major Qualifying Project Report

Submitted to the Faculty of

WORCESTER POLYTECHNIC INSTITUTE

In partial fulfillment of the requirements for the

Degree of Bachelor of Science

By:

Katarina Lopez

April 28, 2011

Approved by:

Prof. Robert E. Connors, Ph.D

Project Advisor

Table of Contents

List of Figures

List of Tables

Abstract

This project extends interest into the photophysical properties of symmetrically substituted 2,5 – diarylidene cyclopentanone dyes. The focus for this research is on the compound (2E,5E)-2,5-bis(4-methoxycinnamylidene)-cyclopentanone (2dbmxcp). This compound was synthesized via a crossed aldol condensation reaction between cyclopentanone with (E)- 4 – methoxycinnamaldehyde in the presence of NaOH. The electronic absorption and fluorescence properties were investigated in a variety of nonpolar, polar protic, and aprotic solvents. Solvatochromic shifts, specifically bathochromic (red) shifts were observed in both the absorption and fluorescence spectra as a result of solvent polarity. In addition to the spectroscopic properties, the photophysical properties were also investigated. This involved calculating the fluorescence quantum yields, and measuring the fluorescence lifetime parameters. The fluorescence quantum yields of 2dbmxcp ranged from 0.0012 in carbon tetrachloride, to 0.17 in 2-propanol. This range was of particular interest because a higher quantum yield in alcohols differs from analogous compounds. First-order radiative and nonradiative rates of decay were determined. Quantum chemical calculations were performed on 2dbmxcp at the DFT B3LYP/6-31G(d) level of theory for geometry optimization and TD-DFT spectral calculations.

Acknowledgements

I would like to thank Professor Robert E. Connors for advising me during the course of the project and for the use of his time, laboratory, and equipment. I would also like to thank Christopher Zoto for all his guidance, patience, and time.

Introduction

Conjugated compounds contain carbon-carbon double bonds in a 1,3 – conformation; a conjugated system is dependent on the overlap of p atomic orbitals. The class of organic conjugated compounds that are of interest for this study is the 2,5 – diarylidene cyclopentanone dyes. These highly conjugated fluorescent dyes have received attention for their large scope of applications. These compounds have been utilized as photosensitizers[3], fluorescent solvent polarity probes[4,5], fluoroionophores[6], and nonlinear optical materials[7].

A recent application of these fluorescent compounds is a technology that has been developed by Constellation 3D known as the fluorescent multilayer disc (FMD). This is an optical disc that uses fluorescent compounds as digital receptors instead of the normal digital reflection used in traditional optical discs to store data. Fluorescent compounds are filled into the pits of an FMD, and light is able to travel through the clear FMD discs unimpeded. This enables the disc to carry up to approximately 100 data layers, much larger than the traditional 2 layers on a normal disc. As a result of the ability of the fluorescent compounds to achieve possible excitation to higher order energy states, the FMD technology can have capacities of up to a terabyte while maintaining the same physical size of a traditional optical disc[8].

Previous research on 2,5 – diarylidene cyclopentanones suggest that they could draw attention for feasible applications in several new technologies. The research conducted by Connors and Ucak-Astarlioglu[1] report the electronic structure and spectroscopic properties for a set of unsubstituted 2,5 – diarylidene cyclopentanones in a variety of solvents; the generic chemical structure of the dye is shown in Figure 1. The research has a primary focus that involves studying the electronic absorption and fluorescence properties of all the trans configurations of unsubstituted 2,5 – diarylidene cyclopentanones (R=H) with n = 1, 2, and 3[1].

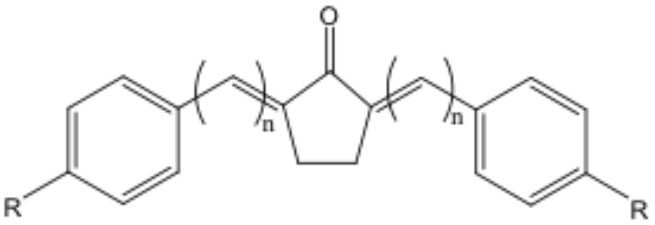

Figure 1. General Structure of 2,5-diarylidene cyclopentanones.

This project serves as an extension of previous research, and it involves studying a derivative with methoxy substituted groups (-OCH_3) (that serve as electron donating groups) bonded at the para positions on the phenyl rings. The spectroscopic and photophysical spectroscopic properties of (2E,5E)-2,5-bis(4-methoxycinnamylidene)-cyclopentanone (2dbmxcp) have been studied in a variety of fourteen nonpolar, polar aprotic, and protic solvents. The chemical structure of 2dbmxcp is shown below in Figure 2. Investigation of the spectroscopic characteristics of 2dbmxcp provide valuable insight into the solvatochromic and photophysical properties of the compound in various solvent systems.

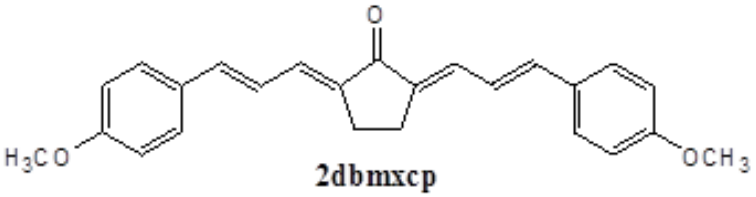

Figure 2. Structure of (2E,5E)-2,5-bis(4-methoxycinnamylidene)-cyclopentanone (2dbmxcp).

Solvatochromism is the ability of a substance to change color with respect to solvent polarity[2]. In absorption and fluorescence spectra, a molecule that exhibits solvatochromic properties undergoes either bathochromic (red) shifts or hypsochromic (blue) shifts depending on the solvent polarity. Past solvatochromic research of analogous dyes show a bathochromic shift when testing from nonpolar to polar aprotic solvents[1]. A Jablonski state energy-level diagram can be used to explain the spectral shifts. This diagram (Figure 3) illustrates the electronic energy states of a molecule and the transitions between them.

More specifically, the diagram is used to show the radiative process of absorption and fluorescence with nonradiative solvent relaxation. Investigation of the solvatochromic properties of 2dbmxcp show that there is a bathochromic (red) shift as the solvent polarity increases.

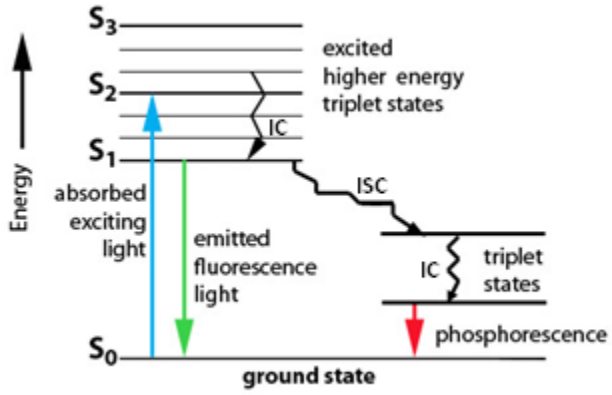

Figure 3. Jablonski diagram showing fluorescence with solvent relaxation[10].

The primary objective for this project is to investigate and analyze the spectroscopic and photophysical properties of 2dbmxcp in various solvents, and explain the trends observed. Examination of the photophysical properties involve experimentally determining the absorption and fluorescence spectra, fluorescence quantum yields (Φ_f), and fluorescence lifetimes (τ_f).

Quantum chemical calculations were performed on 2dbmxcp at the DFT B3LYP/6-31G(d) level of theory. Theoretical calculations consisted of running geometry optimization, TD-DFT spectral calculation, and solvent calculations using the self-consistent reaction field polarizable continuum model (SCRF PCM).

Experimental Procedures

1. Synthesis of (2E,5E)-2,5-bis(4-methoxycinnamylidene)-cyclopentanone (2dbmxcp)

2dbmxcp was synthesized previously and ready for testing at the start of the project. Although the synthesis was not conducted in this project, a look at how the molecule was synthesized provides valuable insight to the structure and composition of 2dbmxcp.

The compound 2dbmxcp was synthesized via a crossed aldol condensation reaction between cyclopentanone (1 mol eq) with (E)-4-methoxycinnamaldehyde (2 mol eq) in the presence of NaOH (see Figure 4). An orange-colored solid precipitated out of solution. The crude material was collected by vacuum filtration and recrystallized from toluene, yielding lustrous orange crystals. ^{1}H NMR spectroscopy was used for structural identification of 2dbmxcp. Both ^{1}H NMR in $CDCl_3$ and IR spectral data are presented in Figures 5-7. Purity was confirmed by TLC (showing one spot upon development).

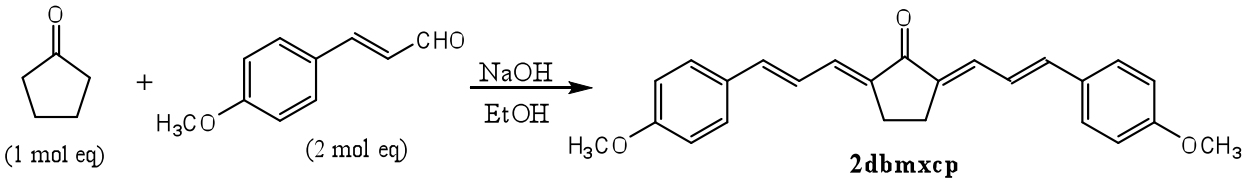

Figure 4. Reaction scheme for the synthesis of 2dbmxcp.

[1]H NMR Spectra of **2dbmxcp** (for structural confirmation)

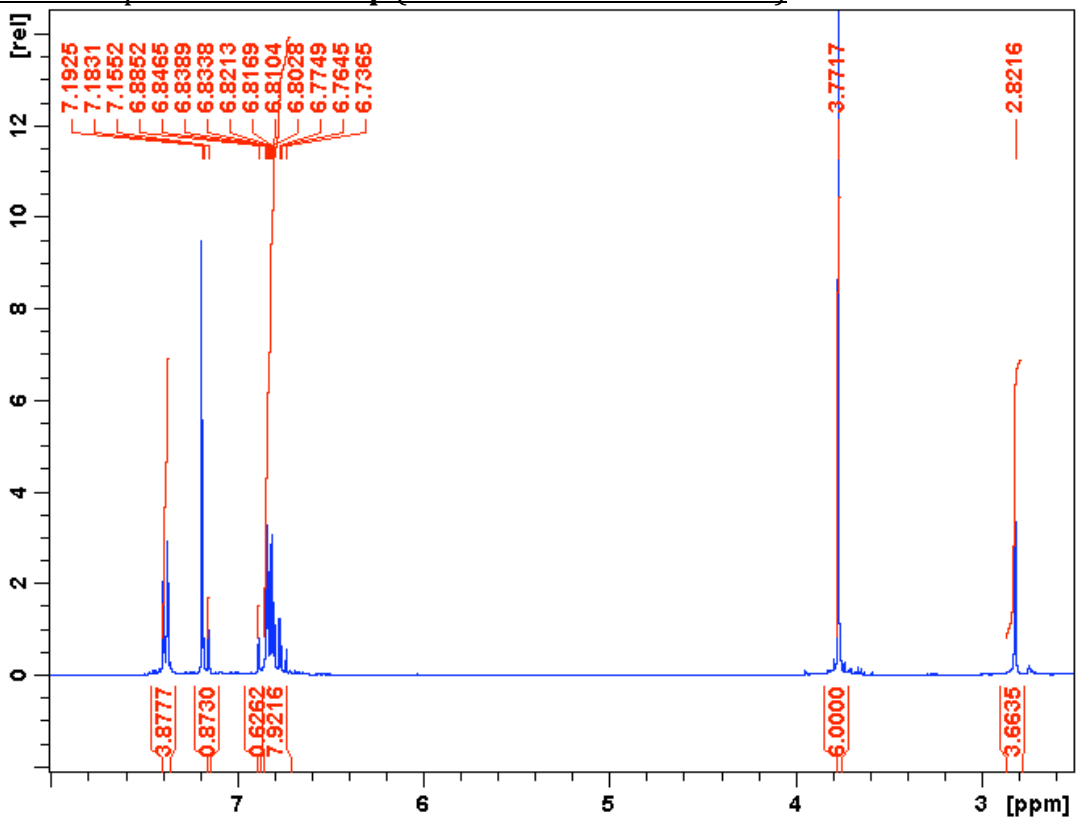

Figure 5: [1]H NMR 2dbmxcp d 2.5-8.0 ppm

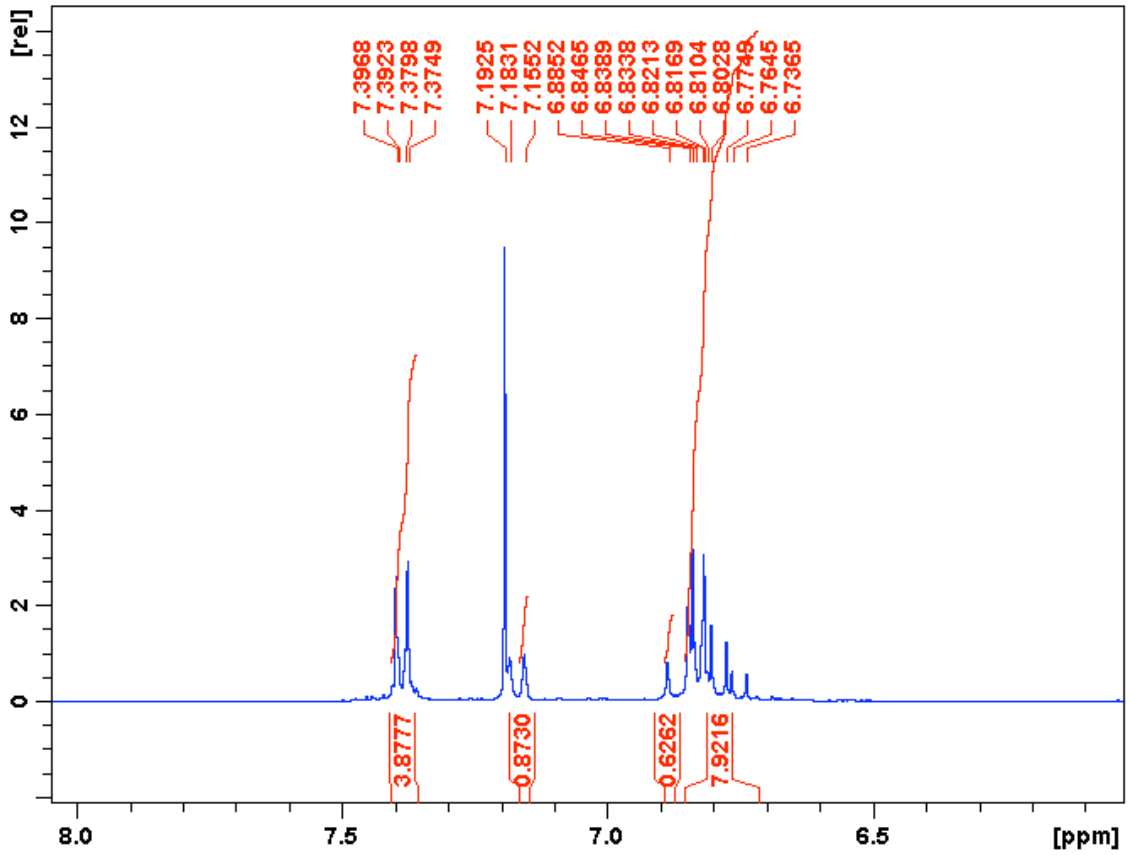

Figure 6: ^{1}H NMR 2dbmxcp d 6.0-8.05 ppm

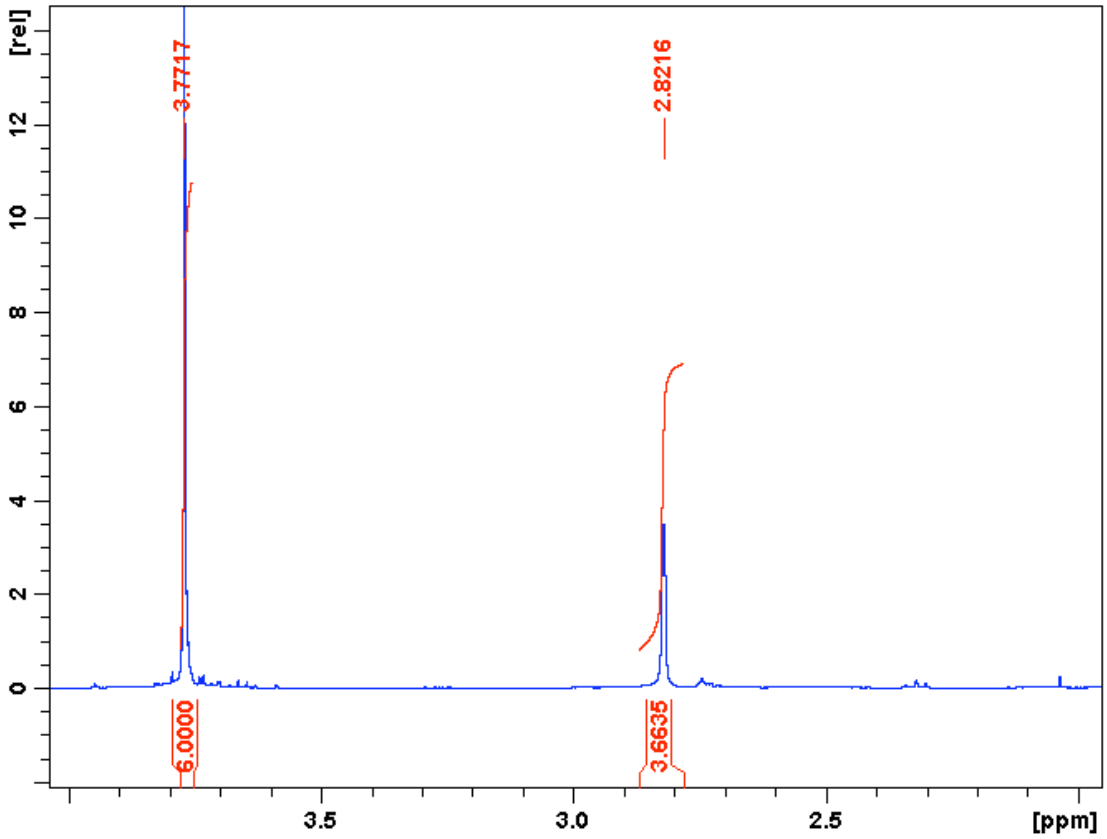

Figure 7: ^{1}H NMR 2dbmxcp d 1.95-4.05 ppm

2. Spectrophotometric Analysis – Absorbance and Fluorescence Spectra

The UV/VIS absorption spectra were measured with a Perkin Elmer® Lambda 35 UV/VIS spectrometer (2 nm band-pass). The fluorescence emission spectra were collected using a Perkin Elmer® LS 50B luminescence spectrophotometer equipped with an R928 phototube detector.

3. Fluorescence Quantum Yield Determination

The fluorescence yield of a compound (Φ_f) is defined as the ratio of photons emitted to the number of photons absorbed by the compound, and can be calculated by the following equation:

$$\Phi_c = \Phi_s \frac{A_s}{A_c} \frac{n_c^2}{n_s^2} \frac{D_c}{D_s} \qquad \text{(Eq. 1)}$$

In this equation, Φs is the fluorescence quantum yield of the known standard (obtained from literature), A is the absorbance value at a fixed wavelength of excitation, n is the refractive index of the solvents used, and D is the calculated area under the corrected emission spectrum. The subscript **s** refers to the standard, and the subscript **c** refers to the compound being investigated.

The fluorescence quantum yields of 2dbmxcp were calculated by preparing two stock solutions of the compound and a solvent with a maximum absorbance of 0.5. Two stock solutions were made in order for the procedure to be performed twice for reproducibility. Absorption was measured using solvents of differing polarities ranging from polar protic, polar aprotic, and nonpolar solvents. All of the solvents were commercially available and spectrophotometric grade. The solvents used were: methanol, ethanol, n-butanol, 1-propanol, 2-propanol, chloroform, dimethyl sulfoxide, acetonitrile, acetone, ethyl acetate, dichloromethane, toluene, benzene, and carbon tetrachloride.

The stock solutions were then diluted ten fold and the optical absorption spectra of both the stock solutions and the diluted solutions were collected. The fluorescence emission spectrum of the tenfold dilutions were recorded, fixing the excitation wavelength

at λ=450 nm. Absorption and fluorescence emission spectra were obtained for all fourteen standard stock solutions, and fluorescein in 0.1 M NaOH (Φf = 0.95)[9]. The diluted fluorescein solution was re-measured for each solvent in order to keep the data consistent, and to account for instrument response. Microsoft Excel® was used to convert spectral data from wavelength units to wavenumbers. The data was then imported into Mathcad®, which was used to correct the fluorescence emission spectra and compute the fluorescence quantum yields. Appendix A illustrates an example of a fluorescence quantum yield calculation for 2dbmxcp in chloroform.

In order to correct the fluorescence emission spectra for instrument response, the literature emission spectrum of N,N-dimethylamino-3-nitrobenzene (N,N-DMANB) was compared to the experimental emission spectrum of N,N-DMANB measured using the LS-50B status. Scale factors were determined every 50cm^{-1} between 12,500 and 22,200 cm^{-1}. [9]

4. Fluorescence lifetime determination

The fluorescence lifetime of a compound (τ_f) is defined as the inverse of the sum of the first-order radiative and nonradiative rates of decay:

$$\tau_f = 1/(k_f + k_{nr}) \qquad \text{(Eq. 2)}$$

where $k_{nr} = k_{ic} + k_{isc}$. The fluorescence lifetimes (τ_f) of 2dbmxcp were measured in the following five solvents: ethanol, 1-propanol, acetone, chloroform, and toluene. Fluorescence lifetimes of 2dbmxcp were measured using a Photon Technology International fluorescence lifetime spectrometer equipped with a GL-3300 nitrogen laser and GL-302 dye laser compartments. In order to prevent fluorescence quenching by oxygen, the solutions were properly degassed by purging with nitrogen prior to measuring the fluorescence decay curves. FeliX 32 computer software was used to generate the time-dependent fluorescence decay spectra. The fluorescence decay profile of the instrument response function (IRF) was generated at the same maximum intensity as the decay curve of the compound being investigated. Ludox (Aldrich), a colloidal suspension of silica, was used as the IRF to scatter the excitation beam. Neutral density filters were used to adjust

the fluorescence intensity of the IRF profile. The fluorescence decay and IRF scatter data were analyzed using a curve-fitting procedure. The best-fit curves were determined by statistically analyzing how well the field fit curve fitted the decay sample curve. An example worksheet for the fluorescence lifetime determination can be found in Appendix B.

Results and Discussion

1. Introduction

The electronic absorption and fluorescence properties of 2dbmxcp were studied in a variety of fourteen polar protic, polar aprotic, and nonpolar solvents. Experimental data show that the solvatochromic properties exhibit a bathochromic (red) shift in color when going from nonpolar to polar solvents. This shift in spectra is illustrated in Figure 9. The resulting solutions differed in color, ranging from lime green, to light green, to yellow, and then to orange with respect to an increase in solvent polarity; illustrating the solvent's influence on light absorption. The absorption and fluorescence properties were measured, and photophysical properties were investigated, which involved measuring fluorescence quantum yields and fluorescence lifetimes in various solvents. Both the first-order radiative and nonradiative rates of decay were calculated from the quantum yield and lifetime data in ethanol, 1-propanol, toluene, acetone, and chloroform. Finally, quantum chemical calculations were performed on 2dbmxcp at the DFT B3LYP/6-31G(d) level of theory, which involved carrying out geometry optimization in the gas phase, along with TD-DFT spectral calculations modeled in the gas phase, and in ethanol and toluene environments.

In order to gain a better understanding of the experimental results and characteristics found from 2dbmxcp, this section will do a comparison study with an analogous compound, 2,5-bis(p-dimethylaminocinnamylidene)-cyclopentanone (2dbma). 2dbma is also a 2,5 – diarylidene cyclopentanone dye, and it also contains electron donating groups (dimethylamino) substituted on the aryl moieties. Figure 8 shows the chemical structure of 2dbma.

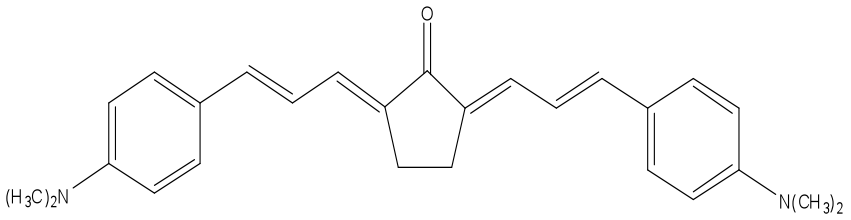

Figure 8. Chemical Structure of 2dbma

2. Absorption and Fluorescence Properties

The absorption and fluorescence spectra of 2dbmxcp in six solvents are shown in Figure 9. This figure illustrates the solvatochromic properties of the compound, and shows that the compound undergoes bathochromic shifts when going from nonpolar, to polar aprotic and protic solvents. Figure 9 shows that there is a more pronounced red shift in the fluorescence spectra than that in the absorbtion spectra. 2dbmxcp shifts in the fluorescence spectra from 518 nm in CCl_4 to 620 nm in MeOH. An interesting experimental finding was that the compound has high fluorescence quantum yield in the polar protic solvents, which was uncharacteristic of analogous dyes. Typically fluorescence signal intensity is lower in polar protic solvents due to the quenching of the compound in the solvent.

The spectroscopic and photophysical characteristics of 2dbmxcp are presented in Table 1. Also included in the table are the solvent polarity function (Δf) and the empirical scale of solvent polarity ($E_T(30)$) of each solvent, which are empirical values based on literature[2]. The solvent polarity function (Δf) is dependent on both the dielectric constant (ε) and the refractive index (n) of the solvent. This relationship is given by:

$$\Delta f = \frac{\varepsilon - 1}{2\varepsilon + 1} - \frac{n^2 - 1}{2n^2 + 1} \qquad \text{(Eq. 3)}$$

The $E_T(30)$ empirical solvent polarity scale is based on the charge transfer shift of the first maximum of a betanine dye[2].

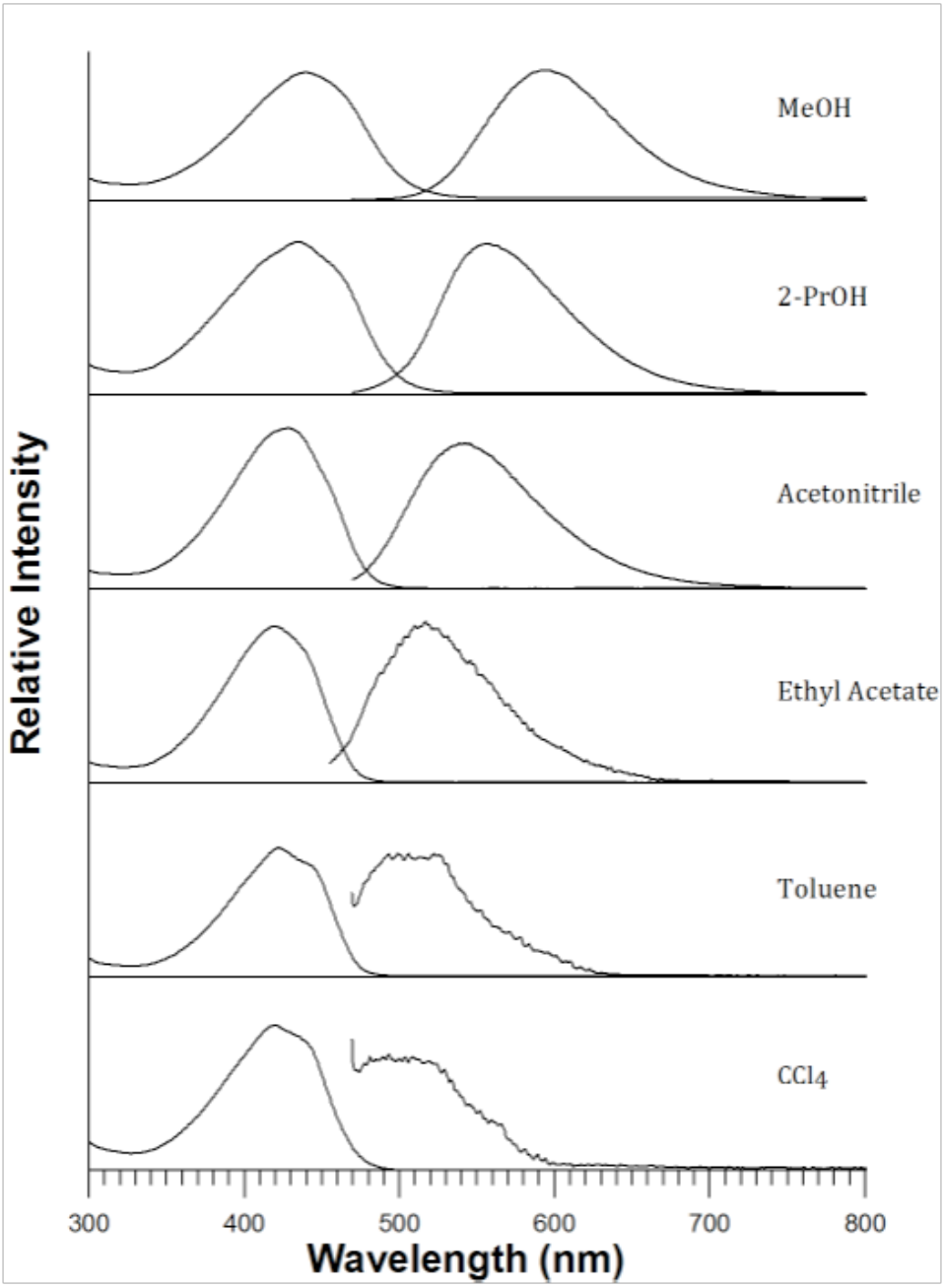

Figure 9. Absorbance and emission spectra of 2dbmxcp in various solvents.

Table 1. Spectroscopic and photophysical characteristics of 2dbmxcp in various solvents.

Solvent	ν_{abs} (cm^{-1})	ν_{flu} (cm^{-1})	Δf*	$E_T(30)$* (kcal mol^{-1})	φ_f	τ_f (ns)	k_f (s^{-1})	k_{nr} (s^{-1})
MeOH	22831 (438 nm)	16119 (620 nm)	0.3093	55.4	0.15	---	---	---
EtOH	22831 (438 nm)	16689 (599 nm)	0.2887	51.9	0.15	0.71	$2.08x10^8$	$1.20x10^9$
1-PrOH	22779 (439 nm)	16813 (595 nm)	0.2746	50.7	0.15	0.72	$2.08x10^8$	$1.18x10^9$
1-BuOH	22727 (440 nm)	18620 (537 nm)	0.2642	50.2	0.08	---	---	---
2-PrOH	23202 (431 nm)	17098 (585 nm)	0.2769	48.4	0.17	---	---	---
DMSO	22779 (439 nm)	17392 (575 nm)	0.2637	45.1	0.16	---	---	---
ACN	23419 (427 nm)	17558 (570 nm)	0.3054	45.6	0.07	---	---	---
Acetone	23529 (425 nm)	17696 (565 nm)	0.2843	42.2	0.04	0.46	$1.00x10^8$	$2.07x10^9$
DCM	23095 (433 nm)	18580 (538 nm)	0.2171	40.7	0.07	---	---	---
Chloroform	22989 (435 nm)	18561 (539 nm)	0.1491	39.1	0.09	0.53	$1.74x10^8$	$1.71x10^9$
EtOAc	23923 (418 nm)	18903 (529 nm)	0.1996	38.1	0.02	---	---	---
Benzene	23641 (423 nm)	18979 (527 nm)	0.0031	34.3	0.005	---	---	---
Toluene	23753 (421 nm)	18979 (527 nm)	0.0131	33.9	0.003	0.27	$1.18x10^7$	$3.69x10^9$
CCl_4	23810 (420 nm)	19302 (518 nm)	0.0119	32.4	0.001	---	---	---

*[2]Both Δf and E_T (30) values were taken from Suppan, P. and Ghonheim, N., in *Solvatochromism,* The Royal Society of Chemistry, Cambridge, 1997.

The absorption and fluorescence characteristics were plotted against both the Δf and the $E_T(30)$ empirical solvent polarity scales, as illustrated in Figures 10 and 11. The figures show that solvatochromic properties are observed, for both the Δf and the $E_T(30)$, having both the absorption and fluorescent wavenumbers decreasing with respect to solvent polarity. The decrease is more prevalent in the $E_T(30)$ scale, whereas the Δf Figure shows only a very slight decrease, signifying only minor solvatochromism.

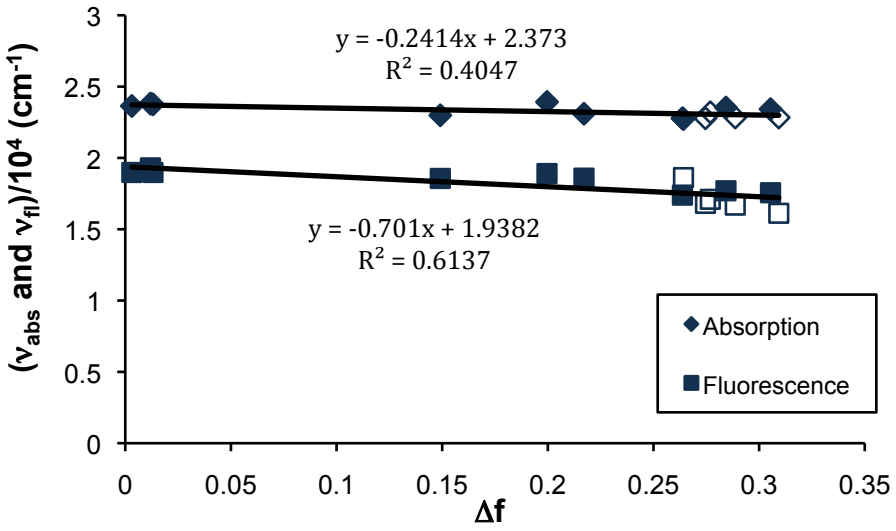

Figure 10. Plot of maximum absorption and fluorescent wavenumbers if 2dbmxcp against Δf in polar protic, polar aprotic, and nonpolar solvents. Alcohols are represented as the clear diamond and square shapes.

In the case of 2dbma, the compound exhibited stronger solvatochromic properties, resulting in a line with greater slope. The observed solvatochromic properties in 2dbma were consistent with a charge transfer electronic transition.

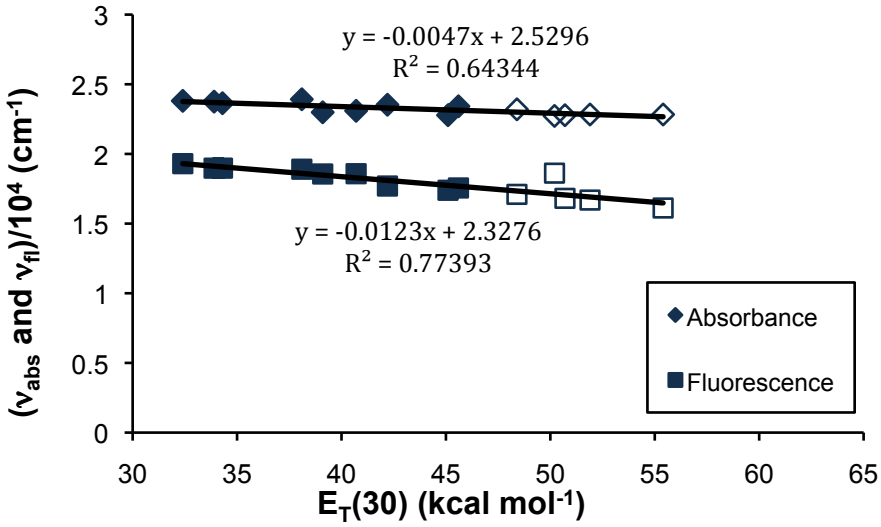

Figure 11. Plot of maximum absorption and fluorescent wavenumbers of 2dbmxcp against $E_T(30)$ in various solvents. Alcohols are represented as clear diamond and square shapes.

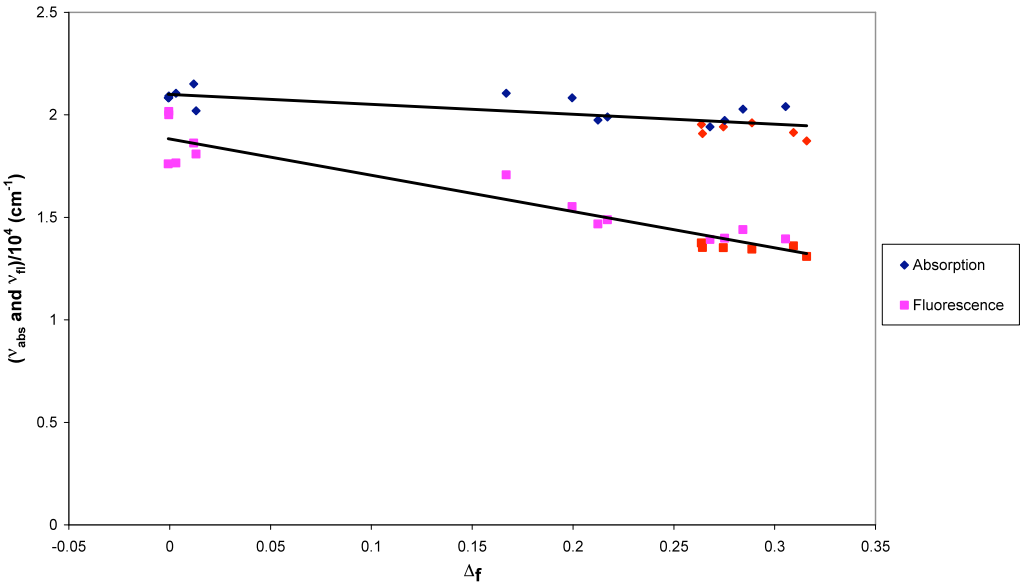

Figure 12. Plot of maximum absorption and fluorescent wavenumbers of 2dbma against Δf in various protic, aprotic, and nonpolar solvents. Alcohols are designated by the red shaped diamonds and squares.

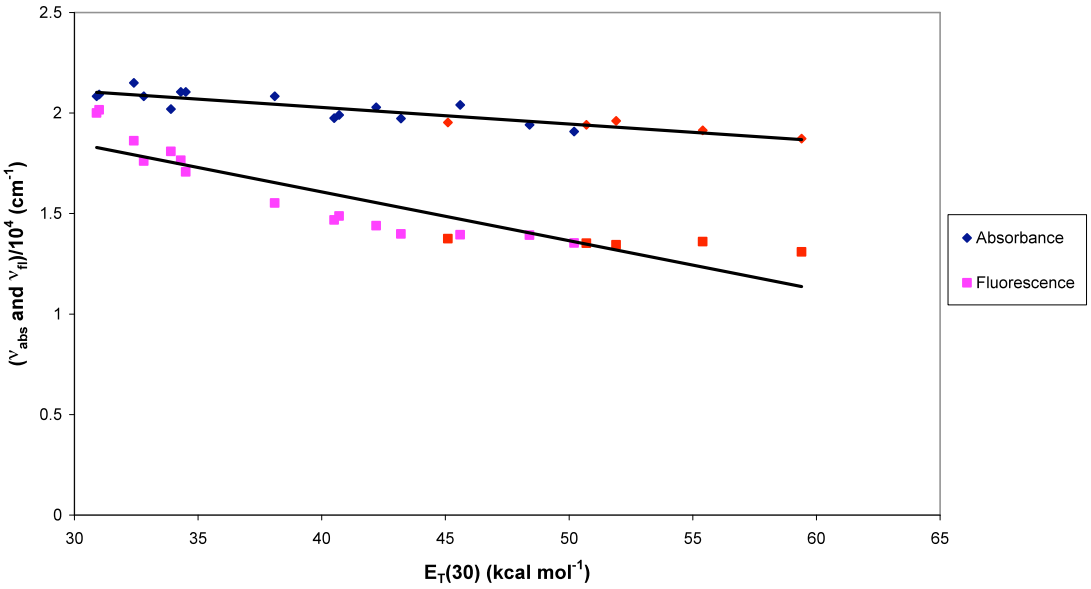

Figure 13. Plot of maximum absorption and fluorescent wavenumbers of 2dbma against $E_T(30)$ in various types of solvents. Alcohols are represented by the red shaped diamonds and squares.

Experimental results from the fluorescence lifetimes (τ_f) and fluorescence quantum yields (Φ_f) show a solvent dependence for the 2dbmxcp. An observation that was made is that the lifetimes and quantum yields changed proportionally from one solvent to another. The alcohols had the highest quantum yields out of the entire solvent set, and were experimentally determined (out of the five solvents tested) to have the highest lifetimes values. The lifetime values are listed in Table 1, and the range of lifetimes went from 0.27 ns in toluene to 0.72 ns in 1-propanol.

The Φ_f and τ_f parameters were used to calculate the first-order radiative (k_f) and nonradiative decay constants of the first excited singlet state of 2dbmxcp. The first-order radiative decay constant can be calculated by the following equation:

$$k_f = \frac{\Phi_f}{\tau_f} \qquad \text{(Eq. 4)}$$

where Φ_f is the fluorescence quantum yield and τ_f is the fluorescence lifetime of the decaying sample. The first order-nonradiative decay constant (k_{nr}), can be calculated from the following equation:

$$k_{nr} = \left(\frac{1}{\Phi_f} - 1 \right) k_f \qquad \text{(Eq. 5)}$$

Although only five fluorescence lifetimes were measured, the k_{nr} appeared to generally decrease as the solvent polarity increased. As shown in Table 1, the k_{nr} went from 3.69×10^9 s^{-1} in toluene to 1.20×10^9 s^{-1} in ethanol. The enery gap law is used to predict the exponential dependence of k_{ic} (internal conversion) on ΔE, the energy gap between S_0 and S_1. This law is expressed by the following equation:

$$k_{ic} = Ce^{-\alpha \Delta E}, \Delta E = E_{S_1} - E_{S_0} \qquad \text{(Eq. 6)}$$

where C and α are constants. In accordance with the energy gap law of internal conversion for excited states, k_{nr} is expected to increase as the evergy gap between S_0 and S_1 decreases due to vibrational overlap between the S_0 and S_1 states. When the S_0 to S_1 energy gap increases, the vibrational overlap between the energy levels of S_0 and S_1 decreases, thus yielding a decrease in the rate of internal conversion. Essentially, this equation states that as k_{ic} increases as ΔE decreases, and thus Φ_f decreases, assuming k_{isc} and k_f are constant. With 2dbma the behavior of k_{nr} can be explained by the energy gap law, but with 2dbmxcp, the higher quantum yields show anti-energy gap behavior.

The fluorescence quantum yields were plotted against the maximum fluorescent wavenumbers (ν_{fl}) in a variety of polar protic, polar aprotic, and nonpolar solvnets, shown in Figure 14.

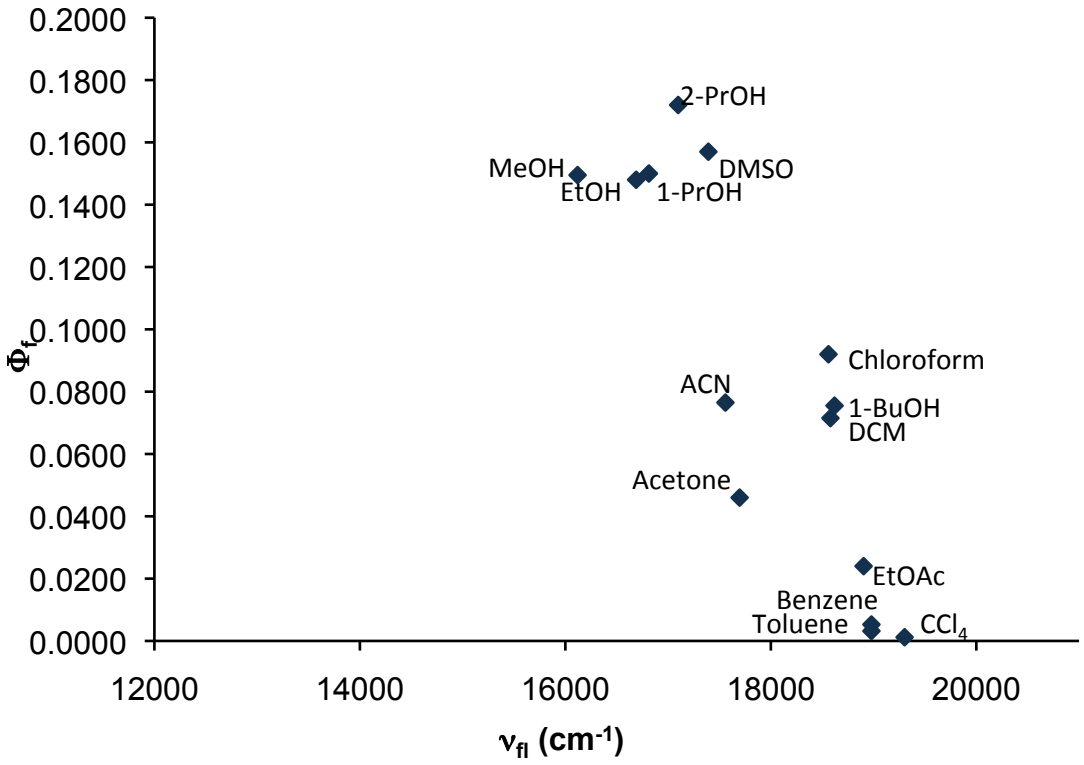

Figure 14. Plot of the fluorescence quantum yield of 2dbmxcp against ν_{fl} in all solvents.

Figure 14 illustrates that the quantum yields increase for solvents with the strongest polarity. This is also true for the fluorecence lifetimes, the sovlents with the larger polarity were experimentally proven to have longer fluorscence lifetimes.

Both 2dbmxcp and 2dbma generated similar quantum yields in the high wavenumbers regions, although they did not have the same quantum yields in the alcohols, 2dbmxcp generated higher quantum yields in the alcohols than 2dbma.

For 2dbma the plot of the fluorescence quantum yield against ν_{fl} illustrates a parabolic relationship. It is observed that the quantum yield reaches a maximum for solvents of

moderate polarity, and this observation is consistent with the interpretation of the trend in k_{nr}. Rearrangment of equations 4 and 5 with $\tau_f = 1/(k_f + k_{nr})$, yields an expression for the fluorescence quantum yield of an electronic system:

$$\Phi_f = \frac{k_f}{k_f + k_{nr}} \qquad \text{(Eq. 7)}$$

$$\Phi_f = \frac{k_f}{k_f + k_{ic} + k_{isc}}$$

where $k_{nr} = k_{ic} + k_{isc}$. For 2dbma, the quantum yield is low at low ν_{fl} values. When the polarity of the solvent increases Φ_f increases due to the decreasing rate in intersystem crossing. When the ν_{fl} increases in more polar solvents, the rate of internal converstion increases and proceeds to dominate over the competing decreasing rate of intersystem crossing, resulting in a lower quantum yield, and thus a parabolic trend when plotting Φ_f vs. ν_{fl}. For 2dbma, this trend is supported by the energy gap law.

With 2dbmxcp, the fluorescence quantum yield against ν_{fl} does not illustrate a parabolic relationship, as seen in Figure 14. In this case the rate of internal conversion does not proceed to dominate over the competing rate of interststem crossing in more polar solvents. Due to this anti-energy gap behavior, the plot of Φ_f vs. ν_{fl} only illustrates the decreasing trend in k_{isc}, and thus higher quantum yields are observed in the more polar solvents. This explanation illustrates that the quantum yield depends on the compitition between k_f , k_{ic}, and k_{isc}.

A comparison of 2dbma and 2dbmxcp in solvents of high polarity such as ethanol and methanol can be used to support the explanation of the observed higher quantum yields seen in 2dbmxcp, and also help in explaining the observed anti-energy gap law behavior.

In 2dbmxcp, the ν_{fl} in both MeOH and EtOH is significantly larger than 2dbma, as seen in Table 2. This means that the energy gap between the S_0 and S_1 states is larger which means that the ΔE is larger. When using the enery gap law equation, having a larger ΔE yields a less dominant rate of k_{ic}, and thus a larger quantum yield. Since 2dbma had

smaller ν_{fl} in both MeOH and EtOH, this leads to a smaller ΔE, larger k_{ic}, and thus a smaller quantum yield.

Table 2. Spectroscopic and photophysical properties of both 2dbmxcp and 2dbma in MeOH and EtOH.

2dbmxcp (ν_{fl}, cm^{-1})	2dbma (ν_{fl}, cm^{-1})
MeOH: 16119 (620 nm)	MeOH: 13605 (735 nm)
EtOH: 16689 (599 nm)	EtOH: 13445 (744 nm)

The solvent calculations computationally conducted in ethanol and toluene help explain the low quantum yield and high k_{nr} observed for 2dbmxcp in toluene. This behavior can be attributed to the location of the (n,π*) orbital type and its influence on intersystem crossing. As shown in Figure 15, the k_{isc} for (π,π*) → (n, π*) is significantly larger than the k_{isc} for (π,π*) → (π,π*). This is determined by El Sayed's rule[12], which states that the rate of intersystem crossing is faster and more efficient between two different orbital types than two of the same orbital type. The overall effect is that k_{isc} and k_{nr} decrease as solvent polarity increases, which is working in opposition of the trend observed in k_{ic} caused by the energy gap law. Thus with more polar solvents, such as ethanol, slow k_{isc} occurs which results in a larger quantum yield.

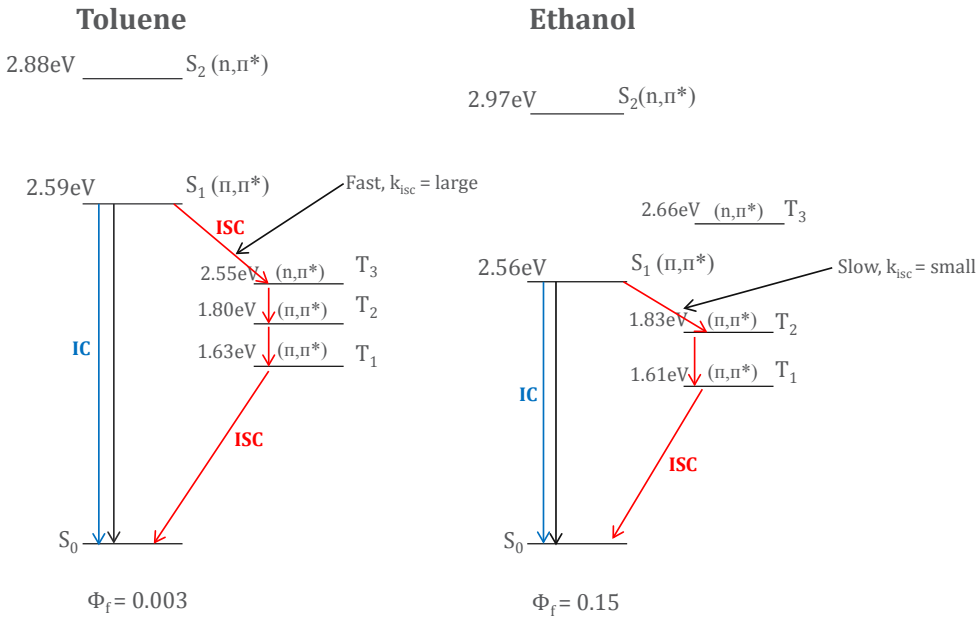

Figure 15. Solvent calculations of 2dbmxcp in Toluene and Ethanol.

Lippert-Mataga Plots were created for 2dbmxcp from the spectroscopic data and are shown in Figures 17, 18, and 19. Figure 17 was constructed with all of the solvents, whereas Figure 18 has just the polar and nonpolar solvents, which yielded a larger R^2 value. Lippert-Mataga plots are used to directly relate the Stoke's shift for a molecule in different solvents to the solvent polarity function. The Stokes shift ($\Delta\nu$), is the energy difference in wavenumbers between the absorption and fluorescence maxima, related linearly to Δf by the Lippert-Mataga equation[11]:

$$\Delta\nu = \frac{2\Delta\mu^2}{hca^3}\Delta f + \Delta\nu_0 \qquad \text{(Eq. 8)}$$

where $\Delta\mu = \mu_e - \mu_g$ is the difference between the excited-state and ground-state dipole moments, h is Plank's constant (6.626×10^{-34}J), c is the speed of light in a vacuum (2.998×10^{8}m s^{-1}) and a is the Onsager cavity radius for the spherical interaction of the dipole in a solvent.

Lippert-Mataga plots create a linear relationship between the stokes shift ($\Delta\nu$) and Δf , yielding a straight line with a slope that is equal to $2\Delta\mu^2/hca^3$. Both a and μ_g are calculated computationally, and are put into the equation to calculate the excited state dipole moment. Computed results yield an Onsager cavity radius equal to 5.86 Å and a ground state dipole moment (μ_g) of 2.04D. Utilizing the Lippert-Mataga calculation method, the excited state dipole moments of 2dbmxcp were calculated to be 10.3D (all solvents), and 11.62D (non-alcohols).

2dbmxcp yields a smaller dipole moment contrary to 2dbma, which gives an excited-state dipole moment of 22.23D. The electronic distribution is internally transferred to a larger degree for 2dbma than 2dbmxcp in going from the ground state to the excited singlet state. This observation is taken from computing the molecular orbitals and the $\Delta\mu$ magnitude between the ground and excited states. So conceptually, it appears that 2dbmxcp would have a smaller charge transfer, due to the small increase in dipole moment.

Additionally, looking at the computed molecular orbitals of 2dbmxcp in comparison to 2dbma shows that there is a clear charge transfer from the homo to the lumo stage in 2dbma. With 2dbmxcp, the charge is transferred to a lesser degree, as shown in Figure 16. According to research conducted by Morimoito[13], fluorescence of an excited molecule with a smaller charge transfer cannot be quenched well by an alcohol because of the weak interaction on the carbonyl oxygen, which is consistent with the results reported here.

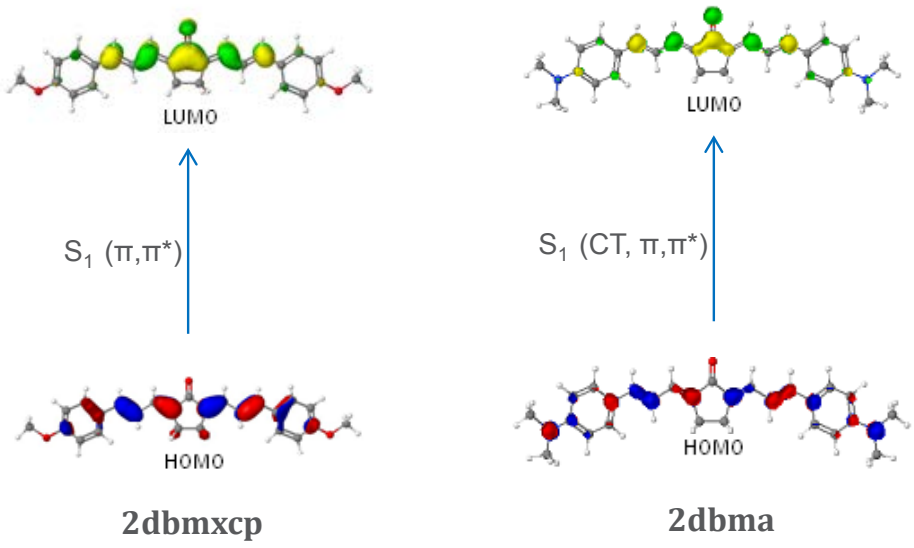

Figure 16. Computed molecular orbitals of 2dbmxcp and 2dbma.

The Lippert-Mataga calculation can be reasoned in a more quantitative way by calculating the unit-charge separation. According to Lacowicz[9], 4.8D is the electronic dipole moment that results from a charge separation of one unit charge by 1 angstrom of length. With that information, if the 11.62 D (non-alcohols) calculation is used, it is comparable to a unit-charge separation of 2.4 angstroms. For 2dbma, the dipole moment of 22.23D is comparable to a unit charge separation of 4.6 angstroms.

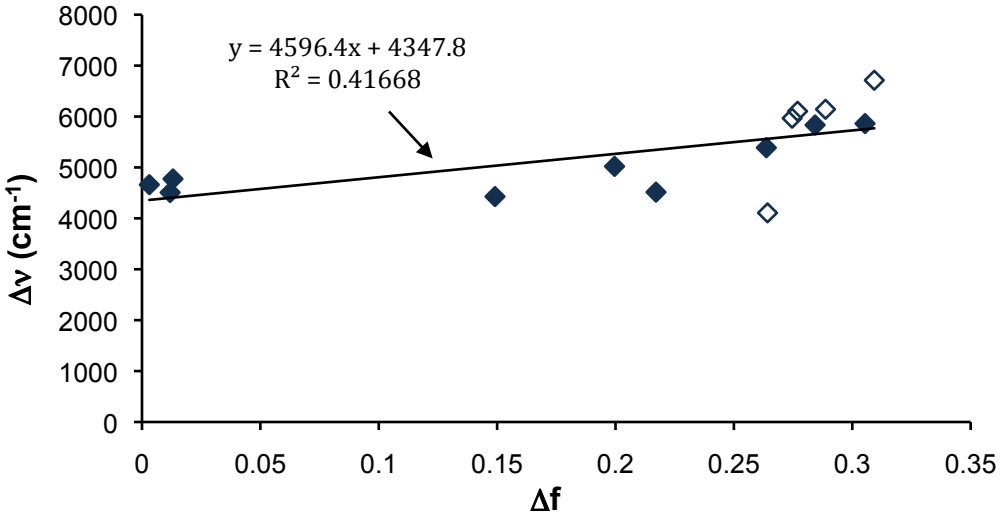

Figure 17. Lippert-Mataga Plot of Stoke's shift (Δν) against Δf of 2dbmxcp in all solvents.

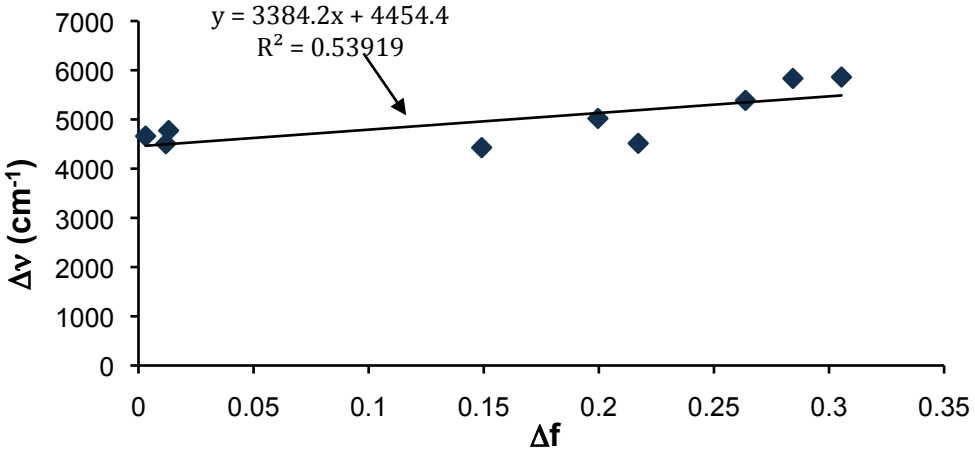

Figure 18. Lippert-Mataga Plot of Stoke's shift (Δν) against Δf of 2dbmxcp in polar protic and nonpolar solvents.

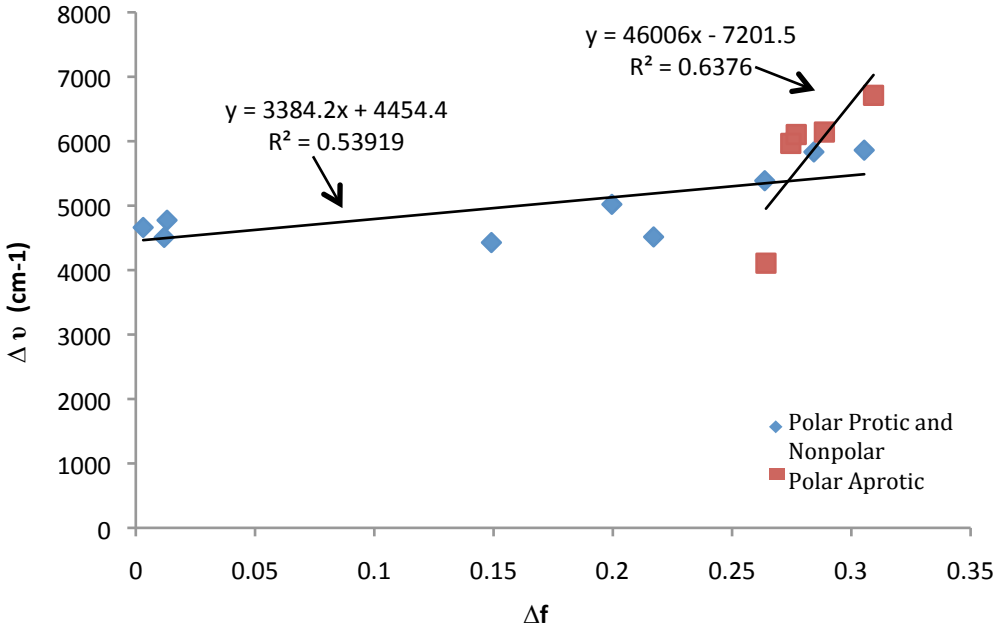

Figure 19. Lippert-Mataga Plot of Stoke's shift (Δν) against Δf of 2dbmxcp in all solvents. Alcohols are designated as the red squares.

3. Quantum Chemical Calculations

DFT B3LYP/6-31G(d) geometry optimization as well as TD-DFT spectral calculations were performed on 2dbmxcp. Molecular orbitals of this compound are shown in Figure 20. Calculations show that the $S_0 \rightarrow S_1$ transition was found to be (π,π^*) and the $S_0 \rightarrow S_2$ transition was predicted to be (n,π^*) Electron density is distributed evenly across the conjugated π system in the computed HOMO, but gets transferred to a minor degree closer to the carbonyl center in the computed LUMO as illustrated in Figure 20. Table 3 shows the molecular orbital calculations of 2dbmxcp as well as the corresponding oscillator strengths (f) for each transition. Table 4 shows the TD-DFT spectral calculations at the B3LYP/6-31G(d) level of theory in ethanol and Toluene.

Table 3. Computed Molecular Orbital Calculations of 2dbmxcp.

HOMO → LUMO	S_1 (π, π^*)
λ=449.72 nm	f=1.9045
HOMO-2 → LUMO	S_2 (n, π^*)
λ = 445.41 nm	f= 0.0000

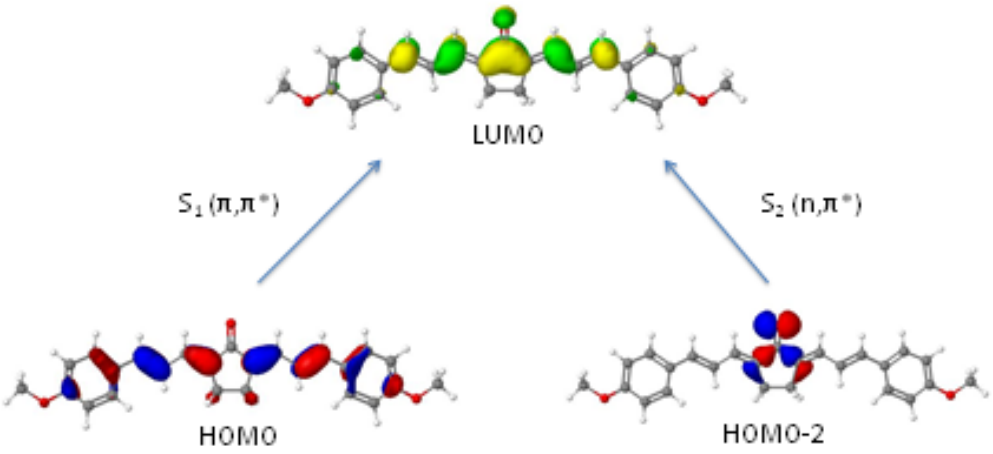

Figure 20. Computed Molecular Orbitals of 2dbmxcp.

Table 4. 2dbmxcp TD-DFT Spectral Calculations in Ethanol and Toluene

Level of Theory: DFT B3LYP/6-31G(d)					
Solvent	Molecular Orbital Calculations		Experimental λ_{max}	Percent Error (%)	Dipole Moment (μ_g)
EtOH	HOMO → LUMO	S_1 (π, π^*)	438 nm		2.78 D
	λ = 483.76 nm	f= 2.1424		9.45	
	HOMO-2 → LUMO	S_2 (n, π^*)			
	λ = 417.49 nm	f=0.0050		4.91	
Toluene	HOMO → LUMO	S_1 (π, π^*)	421 nm		2.38 D
	λ = 478.89 nm	f= 2.1470		12.08	
	HOMO-2 → LUMO	S_2 (n, π^*)			
	λ = 430.84 nm	f=0.0004		2.28	

Conclusions

The experimental results generated from the measured photophysical and spectroscopic properties indicate that 2dbmxcp exhibits solvatochromic properties when tested from nonpolar to polar protic to polar aprotic solvents. 2dbmxcp shows bathochromic (red) shifts, and less red-shifting occurred in the alcohols when compared to an analogous compound 2dbma, signifying less solvatochromism. The spectroscopic characteristics show a linear correlation in both the Δf and $E_T(30)$ scale. 2dbmxcp generated higher quantum yields in the alcohols than 2dbma. This can be attributed to lower solvatochromism, higher ΔE, and lower k_{ic}. These factors combined will produce higher quantum yields. When analyzing the calculated molecular orbital's of 2dbmxcp and 2dbma, there was a clear indication that there was a smaller charge transfer in 2dbmxcp than 2dbma when transitioning from the homo to the lumo. The quantum chemical calculations of 2dbmxcp indicated that S_1 is (π,π*) and S_2 is (n, π*). Additionally it was determined that the quantum yields and fluorescence lifetimes vary upon the nature of the solvent. The most polar solvents exhibited the largest quantum yields and longest lifetimes.

References

1. Connors, R.E.; Ucak-Astarlioglu, M. G. *J. Phys. Chem. A* 2003, 107, 7684.
2. Suppan, P.; Ghonheim, N. *Solvatochromism;* Royal Society of Chemistry: Cambridge, 1997
3. Barnabus, M.V.; Liu, A.; Trifunac, A.D.; Krongauz, V.V.; Chang, C.T. *J. Phys. Chem.* 1992, 96, 212.
4. Pivovarenko, V.G.; Klueva, A.V.;Doroshenko, A.O; Demchenko, A.P. *Chem. Phys. Lett* 2000, 325, 389.
5. Das, P.K.;Pramanik, R.;Banerjee, D.; Bagchi, S. *Spectrochim. Acta. A.* 2000, 56, 2763.
6. Doroshenko, A.O.;Grigorovich, A. V.; Posokhov, E.A.; Pivovarenko, V.G.; Demchenko, A.P. *Mol. Eng.* 1999, *8,*199
7. Kawamata, J.; Inoue, K.; Inabe, T. *Bull. Chem. Soc. Jpn.* 1998, *71,* 2777.
8. Walker, E.P.; Wenyi Feng; Yi Zhang; Haichuan Zhang; McCormick, F.B.; Esener, S.; Call/Recall Inc., San Diego, CA. *3-D Parallel readout in a 3-D multilayer optical data storage system.* Optical Memory and Optical Data Storage Topical Meetingg, 2002. International Symposium. p.147-149
9. Lakowicz, J. R. Principles of Fluorescence Spectroscopy, 2nd ed.; Springer: New York, 2004.
10. "Epi-Fluorescence with the Zeiss Universal." *University of Victoria – Web. UVic.ca.* 21 Sept. 2005. Web. 25 Mar 2011. http://web.uvic.ca/ail/techniques/epi-fluorescence.html.
11. Nad, S.; Pal, H. *J. Phys. Chem. A* 2001, *105*, 1097
12. El-Sayed, M.A. *J. Chem. Phys.* 1963, *38,* 2864.
13. Morimoto, A., Yatsuhashi, T., Shimada, T., Biczok, L., Tryk, D. and Inoue, H. *Radiationless Deactivation of an Intramolecular Charge Transfer Excited State through Hydrogen Bonding: Effect of Molecular Structure and Hard – Soft Anionic Character in the Excited State.* J. Phys. Chem. A 2001, 105, 10488-10496.

Appendix A: Fluorescence Quantum Yield Calculation

Quantum yield determination for 2dbmxcp in Chloroform
with red sensitive tube.
experiment 1

This QuickSheet demonstrates Mathcad' s **cspline** and **interp** functions for connecting X-Y data.

Enter a matrix of X-Y data to be interpolated:
Enter spectral data for compound after converting to wavenumbers, multiplying intensity by lambda squared DO NOT normalize intensity. Insert data from Excel -right key, paste table.

data1 :=

1978.02	$2.52 \cdot 10^6$
21953.9	$2.47 \cdot 10^6$
1929.82	$2.41 \cdot 10^6$
1905.81	...

Click on the **Input Table** above until you see the handles, and enlarge it to see the matrix **data** used in this example.

data1 := csort(data1, 0)

$X := data1^{\langle 0 \rangle}$ $Y := data1^{\langle 1 \rangle}$

Spline coefficients:

S1 := cspline(X, Y)

Fitting function:

fit(x) := interp(S1, X, Y, x)

Sample interpolated values: $fit(21000) = 6.149\times 10^{5}$

$fit(18800) = 8.702\times 10^{6}$

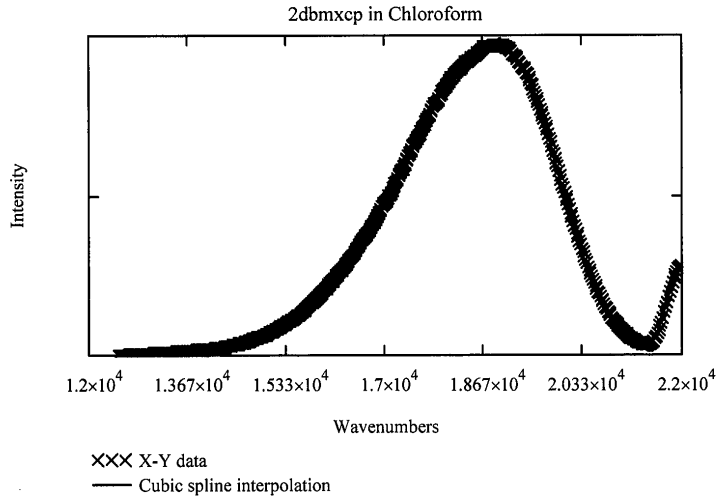

Correction factors for LS50B with red sensitive tube

DATA Limits 12,500-22,200 Wavenumbers

corrdata :=

	0	1
0	12500	4.43
1	12550	...

xdata := csort(corrdata, 0)

A := corrdata⟨0⟩ B := corrdata⟨1⟩

Spline coefficients:

S := cspline(A, B)

Fitting function:

Fitting function:

corrfit(x) := interp(S, A, B, x)

corrspec(x) := corrfit(x)·fit(x)

l := 12500, 12550.. 2220(

l =

1.25·10^4
1.255·10^4
1.26·10^4
...

corrspec(l) =

8.667·10^4
1.753·10^5
1.888·10^5
1.808·10^5
...

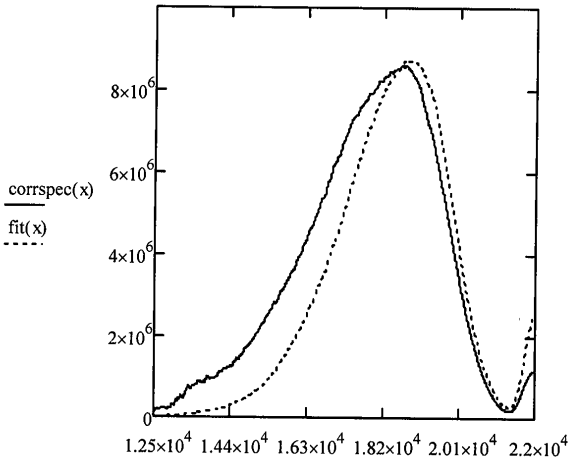

$$\int_{12500}^{21500} \text{fit}(x)\,dx = 2.854\times 10^{10} \qquad \int_{12500}^{21500} \text{corrspec}(x)\,dx = 3.384\times 10^{10}$$

Enter a matrix of X-Y data to be interpolated:

Enter spectral data for standard (fluorescein) after converting to wavenumbers, multiplying intensity by lambda squared DO NOT normalize intensities. Insert data from Excel -right key, paste table.

stdata :=

21978.02	2.55·10^7
21953.9	2.53·10^7
21929.82	...

Click on the **Input Table** above until you see the handles, and enlarge it to see the matrix **data** used in this example.

stdata := csort(stdata , 0)

C := stdata $^{\langle 0 \rangle}$ D := stdata $^{\langle 1 \rangle}$

Spline coefficients:

S := cspline(C, D)

Fitting function:

sfit(x) := interp(S, C, D, x)

sfit(18000) = 1.198×10^{7}

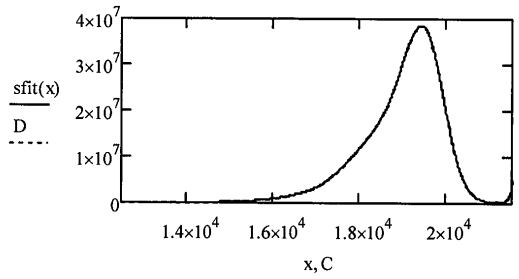

scorrspec (x) := corrfit(x)·(sfit(x))

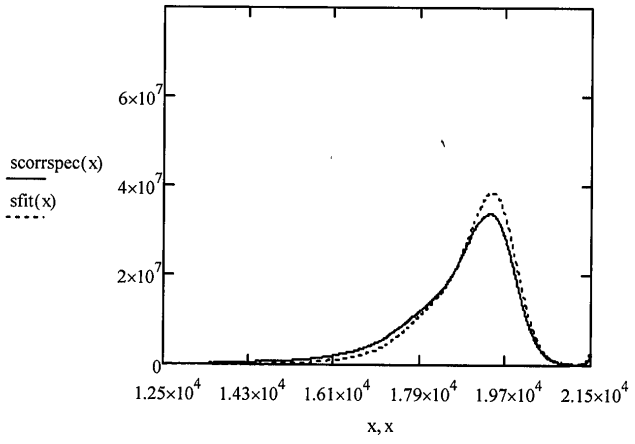

Compound

$$\int_{12500}^{21500} \text{corrspec}(x)\,dx = 3.384\times 10^{10}$$

Standard

$$\int_{12500}^{21500} \text{scorrspec}(x)\,dx = 6.653\times 10^{10}$$

Area under corrected compound curve

$$Dc := \int_{12500}^{21500} \text{corrspec}(x)\,dx$$

$$Dc = 3.384\times 10^{10}$$

Area under corrected standard curve

$$Ds := \int_{12500}^{21500} \text{scorrspec}(x)\,dx$$

$$Ds = 6.653\times 10^{10}$$

	Compound	Standard
Absorbance at (ex)	Ac := 0.04367	As := 0.00817
Index of refraction	CHCl3	NaOH
	nc := 1.445	ns := 1.334
quantum yield of standard		QYs := 0.95

$$QYc := QYs\cdot\left(\frac{As}{Ac}\right)\cdot\left(nc\cdot\frac{nc}{ns\cdot ns}\right)\cdot\left(\frac{Dc}{Ds}\right)$$

$$QYc = 0.106$$

Appendix B: Fluorescence Lifetime Sample Calculation

Fluorescence lifetime calculation of 2dbmxcp in Ethanol

2dbmxcp in Ethanol (sample 1)
****

Analysis Function : Sat Apr 02 2011 at 14:26

****** one-to-four exponentials ******
***** Input Values *****

Decay curve : A1 430:578_s1
IRF curve : normalize(A1 430:430_irfs2)

Start Time : 40.91
End Time : 55.06

Offset will be calculated
Shift will be calculated

Pre-exp. 1 : 1
Lifetime 1 : 1

***** Statistics *****

Job done after 4 iterations in 0.063 sec.

Fitted curve : FLD Fit (2)
Residuals : FLD Residuals (2)
Autocorrelation : FLD Autocorrelation (2)
Deconvolved Fit : FLD Deconvoluted (2)

Chi2 : 2.419
Durbin Watson : 0.5903
Z : -0.1885

Pre-exp. 1 : 1.94 ± 2.365e-002 (100 ± 1.219%)
Lifetime 1 : 0.6975 ± 7.571e-003

F1 : 1

Tau-av1 : 0.6975
Tau-av2 : 0.6975

Offset : 16.63
Shift : -0.184

****